Materials and methods

ES Cell Culture and Differentiation

CGR8 mouse ES cells and ES cells stably transfected with α-myosin heavy chain (MHC) promoter-driven EGFP were cultured as described previously[1], except substituting 15% Knockout Serum Replacement (Invitrogen) for fetal bovine serum. Differentiation was induced by forming embryoid bodies (EB) in the hanging drop suspension culture.[1, 2] SB-431542 was purchased from Tocris. Neutralizing monoclonal antibodies against Activin A and TGF-βs were obtained from R&D systems.

RT-PCR and Immunoblot Analysis

Gene expression was analyzed by semi-quantitative PCR or kinetic real time PCR.[1-3] For sorted cells, total RNA was exacted using RNeasy Micro kit (Qiagen) and analyzed with SuperScript III Platinum SYBR Green One-Step qPCR kit (Invitrogen). The primer sequences and TaqMan Gene Expression Assays used in this study are available upon request. Immunoblot analysis was performed[1, 3] with a primary antibody against Smad1, Smad2/3, TGF-β receptor type II (Millipore), phospho-Smad1/5/8, phospho-Smad2 (Cell Signaling Technology), sarcomeric myosin (MF20;

Developmental Studies Hybridoma Bank), α-actinin (EA-53; Sigma) or GAPDH (Chemicon). For TGF-β receptor type II, the conditioned medium from the cells infected with an adenovirus was analyzed. Densitomeric analysis was performed using ImageJ software.

Replication-defective Recombinant Adenoviruses

Adenoviral vectors expressing a soluble type II TGF-β receptor (sTGF-βIIR), dominant negative mutant of Smad2 or β-galactosidase (LacZ) were prepared as described previously.[4-6] Adenoviral titer was determined by scoring the cytopathic effect in 293T cells using the tissue culture infectious dose 50 method. Cells were infected with adenoviruses at an MOI of 100 in day 0 and at an MOI of 500 in day 5, which produced an almost 100% rate of infection.

Flow Cytometric Analysis and Cell Sorting

α-MHC-EGFP ES cells were dissociated with collagenase type 2 (Worthington), washed, and then immediately analyzed with a FACSCalibur Flow Cytometer using CellQuest acquisition and analysis software (BD Biosciences).[7] Total events of 20,000

were analyzed in each sample. Cell sorting was performed with FACSAria cell sorter using FACSDiva software (BD Biosciences).

Immunostaining

Cells were stained with the primary antibody against sarcomeric α-actinin or βIII-tubulin (Sigma), followed by Alexa Fluor 555-conjugated rabbit anti-mouse IgG secondary antibody (Invitrogen). Nuclear staining was performed with DAPI. For phospho-histone H3 staining, sorted cells were centrifuged onto polylysine slides (Cytospin, Shandon), and stained with anti-phospho-histone H3 antibody (Millipore) and Alexa Fluor 568-conjugated goat anti-rabbit IgG secondary antibody (Invitrogen).

BrdU Incorporation Assay

Cells were labeled with 10 μmol/L BrdU for 2 hours at day 8. After being washed, cells were dissociated with collagenase type 2, sorted, centrifuged onto polylysine slides, fixed in 100% ethanol, and stained with anti-BrdU antibody (Roche) and Alexa Fluor 555-conjugated rabbit anti-mouse IgG.

Statistical Analysis

All experiments were performed at least 3 times, and data were expressed as mean ± standard deviation, and analyzed by Student's *t* test or One-way ANOVA with post hoc analysis. A value of $P<0.05$ was considered statistically significant.

References

1. Takahashi T, Lord B, Schulze PC, Fryer RM, Sarang SS, Gullans SR, Lee RT. Ascorbic acid enhances differentiation of embryonic stem cells into cardiac myocytes. *Circulation.* 2003;107:1912-1916.

2. Hakuno D, Takahashi T, Lammerding J, Lee RT. Focal adhesion kinase signaling regulates cardiogenesis of embryonic stem cells. *J Biol Chem.* 2005;280:39534-39544.

3. Nakajima N, Takahashi T, Kitamura R, Isodono K, Asada S, Ueyama T, Matsubara H, Oh H. MicroRNA-1 facilitates skeletal myogenic differentiation without affecting osteoblastic and adipogenic differentiation. *Biochem Biophys Res Commun.* 2006;350:1006-1012.

4. Ueno H, Sakamoto T, Nakamura T, Qi Z, Astuchi N, Takeshita A, Shimizu K, Ohashi H. A soluble Transforming Growth Factor beta receptor expressed in muscle prevents liver fibrogenesis and dysfunction in rats. *Hum Gene Ther.* 2000;11:33-42.

5. Alvarez J, Serra R. Unique and redundant roles of Smad3 in TGF-β-mediated regulation of long bone development in organ culture. *Dev Dyn.* 2004;230:685-699.

6. Ueyama T, Kasahara H, Ishiwata T, Nie Q, Izumo S. Myocardin expression is regulated by Nkx2.5, and its function is required for cardiomyogenesis. *Mol Cell Biol.* 2003;23:9222-9232.

7. Tateishi K, Ashihara E, Honsho S, Takehara N, Nomura T, Takahashi T, Ueyama T, Yamagishi M, Yaku H, Matsubara H, Oh H. Human cardiac stem cells exhibit mesenchymal features and are maintained through Akt/GSK-3β signaling. *Biochem Biophys Res Commun.* 2007;352:635-641.

Available online at www.sciencedirect.com
ScienceDirect
Biochemical and Biophysical Research Communications 359 (2007) 341–347
BBRC
www.elsevier.com/locate/ybbrc

Osteopontin is a myosphere-derived secretory molecule that promotes angiogenic progenitor cell proliferation through the phosphoinositide 3-kinase/Akt pathway

Takehiro Ogata [a], Tomomi Ueyama [a,*], Tetsuya Nomura [a,b], Satoshi Asada [a,b], Masashi Tagawa [a,b], Tomoyuki Nakamura [c], Tomosaburo Takahashi [a,b], Hiroaki Matsubara [a,b], Hidemasa Oh [a,*]

[a] *Department of Experimental Therapeutics, Translational Research Center, Kyoto University Hospital, Kyoto 606-8507, Japan*
[b] *Department of Cardiovascular Medicine, Kyoto Prefectural University School of Medicine, Kyoto 602-8566, Japan*
[c] *Department of Pharmacology, Kansai Medical University, Moriguchi, Osaka 570-8507, Japan*

Received 11 May 2007
Available online 24 May 2007

Abstract

We have reported that skeletal myosphere-derived progenitor cells (MDPCs) can differentiate into vascular cells, and that MDPC transplantation into cardiomyopathic hearts improves cardiac function. However, the autocrine/paracrine molecules and underlying mechanisms responsible for MDPC growth have not yet been determined. To explore the molecules enhancing the proliferation of MDPCs, we performed serial analysis of gene expression and signal sequence trap methods using RNA isolated from MDPCs. We identified osteopontin (OPN), a secretory molecule, as one of most abundant molecules expressed in MDPCs. OPN provided a proliferative effect for MDPCs. MDPCs treated with OPN showed Akt activation, and inhibition of the phosphoinositide 3-kinase (PI3K)/Akt pathway repressed the proliferative effect of OPN. Furthermore, OPN-pretreated MDPCs maintained their differentiation potential into endothelial and vascular smooth muscle cells. These findings indicate an important role of OPN as an autocrine/paracrine molecule in regulating the proliferative growth of muscle-derived angiogenic progenitor cells via the PI3K/Akt pathway.

Keywords: Osteopontin; Skeletal muscle; Progenitor cells; Proliferation; Differentiation

Studies carried out in the past few years have shown adult skeletal muscle tissue contains stem cells able to differentiate into several lineages [1–5]. We have reported the isolation of multipotent progenitor cells from adult skeletal muscle tissue [6] on the basis of their proliferative potential to form floating-spheres (termed myospheres) [5]. Myosphere-derived progenitor cells (MDPCs) have phenotypic characteristics resembling mesenchymal stem cells and differentiate into endothelial and smooth muscle cells. When MDPCs were grafted into δ-sarcoglycan knockdown hearts that served as a model of cardiomyopathy, neoangiogenesis was enhanced and cardiac function was improved. Since skeletal muscle is an easily accessible tissue source, MDPCs have the potential for clinical application to treat patients with heart failure. For efficient autologous transplantation as a regenerative therapy, sufficient numbers of expanded MDPCs from small tissue samples will be required. However, little is known about the molecules and mechanisms controlling MDPC self-renewal.

In adult neural stem cells (NSCs), a glycosylated form of cystein C [7] and insulin-like growth factor-1 [8] are essential autocrine/paracrine molecules identified as cofactors of basic fibroblast growth factor (bFGF) and epidermal growth factor (EGF), respectively. Stem cell-derived neural

* Corresponding authors. Fax: +81 75 751 4741 (T. Ueyama).
E-mail addresses: tueyama@kuhp.kyoto-u.ac.jp (T. Ueyama), hidemasa@kuhp.kyoto-u.ac.jp (H. Oh).

0006-291X/$ - see front matter © 2007 Elsevier Inc. All rights reserved.
doi:10.1016/j.bbrc.2007.05.104

stem/progenitor cell supporting factor has been also identified as an autocrine/paracrine factor that facilitates the proliferative growth of adult NSCs [9]. Therefore, we anticipated that MDPCs could produce autocrine/paracrine factors that regulate their own proliferative growth. In the present study, we identified osteopontin (OPN, also referred to as secreted phosphoprotein 1), a secreted molecule that promotes the proliferative growth of MDPCs, and clarified the role of the phosphoinositide 3-kinase (PI3K)/Akt signaling pathway in MDPCs treated with OPN.

Materials and methods

MDPC isolation. MDPC isolation was performed as previously described [6]. Briefly, the primary hindlimb muscle cells were isolated from 8-week-old C57BL/6J mice (Shimizu Laboratories Supplies) using 470 U/ml collagenase type II (Worthington) for digestion. Cells were suspended in the isolation medium, which was DMEM/F12 (Invitrogen) supplemented with B27 (Invitrogen), 20 ng/ml EGF (SIGMA), and 40 ng/ml recombinant bFGF (Promega). Cell suspensions were then cultured onto a non-coated dish at 20 cells/μl density over 7 days to generate myospheres.

MDPC expansion and differentiation. Myospheres were picked and transferred into fibronectin-coated culture plates in an expansion medium composed of Advanced DMEM/F12 (Invitrogen), 200 μM L-glutamine (SIGMA), 2% fetal bovine serum (FBS), 20 ng/ml EGF, 10 ng/ml bFGF, and 10 ng/ml LIF (CHEMICON) to obtain MDPCs. Differentiation medium containing DMEM/F12 and 10% FBS supplemented with 10 ng/ml vascular endothelial growth factor (VEGF; R&D Systems) or 50 ng/ml platelet-derived growth factor-BB (PDGF; R&D Systems) was used to induce endothelial or smooth muscle cell differentiation, respectively.

Serial analysis of gene expression (SAGE). The SAGE libraries were constructed essentially following the I-SAGE long kit protocol (Invitrogen) using total RNA extracted from MDPCs. The double-stranded cDNA was digested with NlaIII and the restriction enzyme was replaced by MmeI after linker ligation. Ditags produced from 400 PCRs were isolated, cleaved with NlaIII, and cloned into pZErO. All sequence files were processed using the SAGE2000 ver. 4.5 software. The extracted tags were further processed to determine the identity of associated genes through several stringent filters using the CGAP website (http://cgap.nci.nih.gov/SAGE).

Signal sequence trap (SST). SST was performed as previously described [10,11]. Briefly, a library was constructed in the retrovirus vector pMX-SST employing cDNA derived from mRNA isolated from MDPCs. The interleukin-3 (IL-3)-dependent pro-B cell line Ba/F3 was infected with retrovirus, followed by seeding onto 96-multiwell plates in the absence of IL-3. Genomic DNAs extracted from IL-3-independent Ba/F3 clones were subjected to PCR to recover the integrated cDNAs using primers specific for the cloning vector. After electrophoresis of the PCR products, DNA was recovered and subjected to sequencing.

Immunofluorescent microscopy. Specimens were fixed in 4% paraformaldehyde and stained with rabbit monoclonal anti-OPN antibody (IBL, Fujioka, Japan), rat monoclonal anti-CD31 antibody (BD Biosciences), and mouse monoclonal anti-smMHC antibody (DAKO). Secondary antibodies were conjugated with Alexa Flour 555, and nuclei were visualized using 4′,6-diamino-2-phenylindole (DAPI; Invitrogen).

RNA extraction and quantitative reverse transcriptase (RT)-polymerase chain reaction (PCR). Total RNA was extracted from MDPCs using the RNeasy mini kit (QIAGEN) and cDNA was synthesized by the SuperScript III kit (Invitrogen). Synthesized cDNA was analyzed by kinetic real-time PCR using the ABI Prism 7700 Sequence Detector system (Applied Biosystems) with SYBR Green Real-time PCR Master Mix (TOYOBO, Osaka). Mouse glyceraldehyde-3-phosphate dehydrogenase (GAPDH) was used for normalization, and the comparative threshold (C_T) method was used to assess the relative abundance of the targets. Primers used were as follows: OPN-f, GCAGACACTTTCACTCCAATCG; OPN-r, GCCCTTTCCGTTGTTGTCCTG; GAPDH-f, TTGTGATGGGTGTGAACCACGAGA; GAPDH-r, CATGAGCCCTTCCACAATGCCAAA.

MDPC proliferation assay. To test the proliferative effect of OPN or growth factor on MDPCs, recombinant OPN (R&D Systems), LIF, EGF or bFGF was added to the culture medium. Seventy-two hours after treatment, cell proliferation and/or viability effects were estimated using Cell Proliferation Reagent WST-1 (Roche Applied Science), which was added to the culture medium and measured the number of viable cells. Twenty-four hours after treatment, cell proliferation was also estimated by the measurement of BrdU incorporation into newly synthesized cellular DNA using Cell Proliferation ELISA, BrdU (colorimetric) (Roche Applied Science). To estimate the involvement of the PI3K/Akt pathway, MDPCs were pretreated with 1.0 μM LY294002 (CALBIOCHEM) or 5.0 μM Akt inhibitor (CALBIOCHEM) for 30 min.

Western blotting. Cell lysates were extracted with a lysis buffer containing 50 mM Tris–HCl (pH 7.4), 150 mM NaCl, 1 mM EDTA, 1% Nonidet P-40, 1 mM PMSF, 1× protease inhibitor cocktail (Pierce), 1 mM Na_3VO_4, and 1 mM NaF. Cell lysates were electrophoresed on 10% SDS–polyacrylamide gels and transferred to polyvinylidene difluoride membranes (Millipore). Transferred membranes were incubated with primary antibodies against phospho-Akt (S473) and Akt (Cell Signaling). Horseradish peroxidase (HRP)-conjugated anti-rabbit IgG (GE Healthcare) was used as a secondary antibody.

Statistical analysis. All experiments were performed at least three times. Data were expressed as means ± standard error and analyzed by one-way ANOVA with post hoc analysis. A value of $P < 0.05$ was considered significant.

Results

Identification of osteopontin

To explore the potential molecules regulating MDPC proliferation, we performed SAGE and SST using RNA isolated from MDPCs. SAGE provides a comprehensive approach for elucidation of quantitative gene expression patterns that does not depend on prior availability of transcript information [12], and SST is an efficient strategy to identify secreted and cell-surface molecules [11]. By using the two distinct methods, we identified OPN, a secretory molecule, as one of the most abundant molecules expressed in MDPCs. To confirm OPN expression in MDPCs, we performed immunostaining using an anti-OPN antibody. As shown in Fig. 1A, OPN protein was readily detected in myospheres and individual MDPCs.

When MDPCs were isolated and expanded, we used an isolation medium and an expansion medium, respectively. Both media contain bFGF and EGF, while LIF was also used in the expansion medium. Since bFGF has been reported to increase OPN mRNA expression in rat osteosarcoma cells [13], we speculated that the growth factors used might affect OPN expression during the isolation and expansion of MDPCs. To examine this possibility, quantitative RT-PCR for OPN mRNA was performed using total RNA isolated from MDPCs treated with or without the growth factors. Among the growth factors used in the present study, bFGF enhanced OPN mRNA expression in MDPCs (Fig. 1B), whereas EGF and LIF did not. The addition of exogenous OPN did not alter

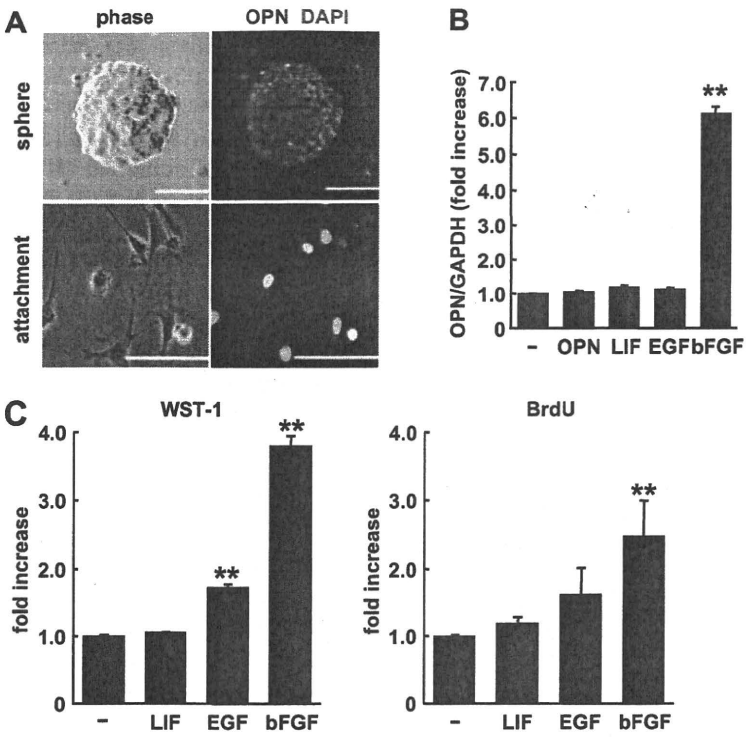

Fig. 1. OPN expression in MDPCs. (A) OPN expression in spheroid or attached MDPCs was examined by immunostaining using an anti-OPN antibody. Bar indicates 200 μm. (B) MDPCs were treated with or without the growth factors for 12 h. OPN mRNA expression in MDPCs was assessed by real-time RT-PCR. Concentrations of LIF, EGF, and bFGF were 10, 20, and 10 ng/ml, respectively. (C) Cell proliferation activity was assessed using the WST-1 and BrdU ELISA assay systems. MDPCs were treated with or without the growth factors. Values are means ± SEM. $^{**}P < 0.01$ vs control.

endogenous OPN mRNA expression in MDPCs, indicating that OPN has no feedback regulation on its own expression. Furthermore, to investigate which of these growth factors contributes to MDPC proliferation, we measured cell proliferation activity by using WST-1 and BrdU ELISA assays (Fig. 1C). Significant increases in the number of viable MDPCs estimated by the WST-1 assay were seen in EGF- and bFGF-treated MDPCs, and increased DNA synthesis measured by the BrdU ELISA assay was detected in bFGF-treated MDPCs, suggesting that both EGF and bFGF have proliferative effects for MDPCs. In contrast, LIF had no obvious proliferative effect on MDPCs.

OPN has a proliferative effect for MDPCs

We then examined the role of OPN on MDPC proliferation. When the recombinant OPN protein was added to the culture medium containing 2% FBS and growth factors (bFGF, EGF, and LIF) to mimic the culture condition for MDPCs expansion, slight but significant increases in the numbers of viable MDPCs and DNA synthesis were observed in 5.0 μg/ml OPN-treated MDPCs as estimated by WST-1 assay and BrdU ELISA assay, respectively (Fig. 2A). Even if FBS was removed from the above medium mimicking the culture condition for MDPC isolation, the addition of OPN at a concentration of 5.0 μg/ml also induced a significant increase in MDPC proliferation (Fig. 2B). These findings suggest that OPN cooperates with bFGF, EGF, and LIF to induce MDPC proliferation during isolation and expansion of MDPCs.

The findings showed in Fig. 1B suggest that OPN is secreted into the culture medium from MDPCs treated with the growth factors. This may have caused additional OPN treatment to show only a slight effect on growth factors-treated MDPC proliferation as shown is Fig. 2A and B. Furthermore, the results obtained above did not reveal whether OPN alone in the absence of the growth factors could have an effect on MDPC proliferation. Therefore, to clarify the proliferative effect of OPN alone, the recombinant OPN protein was added to the culture medium without FBS and the growth factors, and then cell proliferation activity was assessed. As shown in Fig. 2C, OPN significantly increased MDPC proliferation as assessed by the cell number (right panel) and DNA synthesis (left panel) in a dose dependent manner.

The proliferation of MDPCs induced by OPN depends on the PI3K/Akt pathway

OPN has been reported to activate various kinases such as PI3K, nuclear factor inducing kinase, protein kinase C,

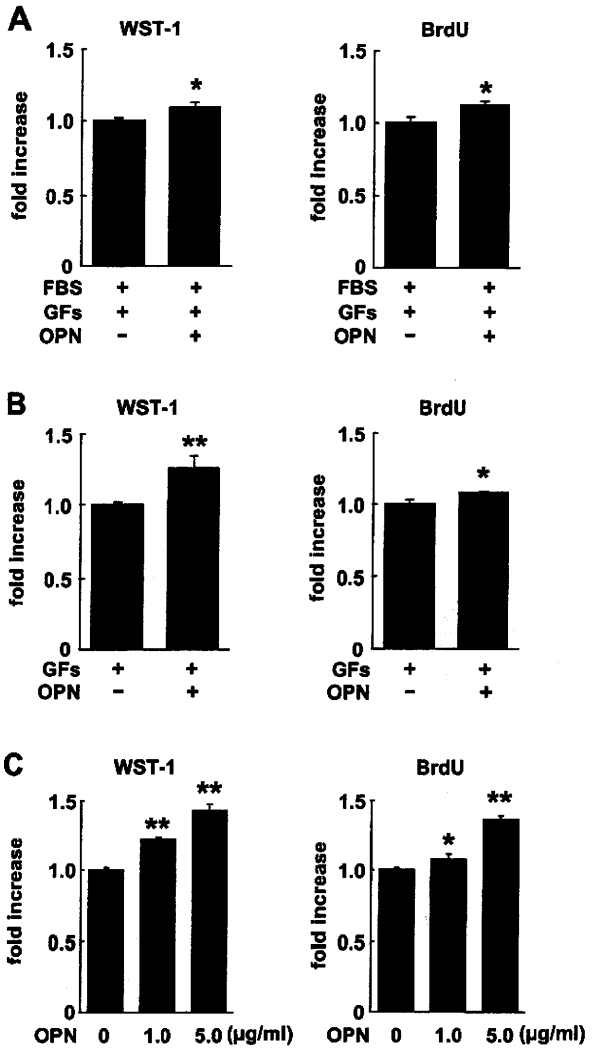

Fig. 2. Enhancement of proliferation effect on MDPCs by OPN. Cell proliferation activity was assessed by use of the WST-1 and BrdU ELISA assay systems. (A) MDPCs were treated with or without 5.0 μg/ml OPN in the culture medium containing 2% FBS and GFs. (B) MDPCs were treated with or without 5.0 μg/ml OPN in the culture medium containing GFs. (C) MDPCs were treated with indicated concentrations of OPN in the culture medium without FBS and GFs. Values are means ± SEM. GFs, growth factor mix (10 ng/ml LIF, 20 ng/ml EGF, and 10 ng/ml bFGF). $^{*}P<0.05$, $^{**}P<0.01$ vs control.

and MAP kinases [14]. Since we have shown that the proliferation of cardiac stem cells (CSCs) is dependent on the Akt pathway [15], we investigated whether OPN induces Akt activation in MDPCs. As shown in Fig. 3A, OPN-induced Akt phosphorylation was detected within 15 min after the addition of OPN, reached a maximum at around 30 min, and then declined. Since Akt is one of downstream target molecules of PI3K, we then examined whether OPN-induced activation of the PI3K/Akt pathway regulates MDPC proliferation. To define the role of the PI3K/Akt pathway, we used inhibitors for PI3K and Akt. OPN-induced Akt phosphorylation was inhibited by 1.0 μM of LY294002, a PI3K inhibitor, and 5.0 μM of Akt inhibitor in MDPCs (data not shown). Therefore, we treated MDPCs with 1.0 μM LY294002 or 5.0 μM Akt inhibitor, followed by the addition of OPN, and then measured cell proliferation activity. As shown in Fig. 3B, pretreatment with LY294002 inhibited OPN-induced MDPC proliferation as assessed by WST-1 and BrdU ELISA assays. Akt inhibition also reduced OPN-induced MDPC proliferation as assessed by WST-1 and BrdU ELISA assays (Fig. 3C). These results indicate that OPN-induced MDPC proliferation depends on the PI3K/Akt pathway.

OPN-treated MDPCs can differentiate into endothelial and smooth muscle cells

Finally, we examined the potential of MDPCs treated with OPN to differentiate into vascular cells. MDPCs that had been treated with 1.0 μg/ml of OPN for 4 days were induced into endothelial and smooth muscle cell differentiation using VEGF and PDGF, respectively. Immunostaining using an anti-CD31 antibody showed that CD31 positive cells appeared by 14 days after treatment with VEGF (Fig. 4, upper panel). When MDPCs treated by OPN were cultured in the differentiation medium containing PDGF for 14 days, smMHC positive cells were observed (Fig. 4, lower panel). These results indicate that OPN-treated MDPCs retained their replicative growth capacity and could maintain the commitment to differentiate into at least two different vascular lineages: endothelial and smooth muscle cells.

Discussion

OPN has been known to be involved in many physiological and pathological processes including cell adhesion, angiogenesis, apoptosis, inflammatory responses and tumor metastasis [16]. Here, we identify OPN as a myosphere-derived secretory molecule, and provide a novel role of OPN in regulating the proliferative growth of MDPCs through the PI3K/Akt signaling pathway.

bFGF and EGF have been revealed to affect the rates of proliferation for neural stem and progenitor cells [17]. Studies from single cell cultures demonstrated that EGF and bFGF are mitogens for neurospheres [18,19]. Both bFGF and EGF were also used for the isolation of CSCs as a cardiosphere from the heart [20]. Muscle-derived stem cells were isolated as a myosphere from skeletal muscle by Sarig et al. using bFGF and LIF [5]. Similarly, we have shown that MDPCs as well as CSCs can be isolated as a sphere and expanded using bFGF, EGF, and LIF [6,15]. Regarding the proliferation of MDPCs, we demonstrated here that proliferative effects were dependent on bFGF and EGF but not LIF, and that the effect of bFGF was greater than that of EGF. The previous report by Sarig et al. showed that LIF increased the proportion of Sca-1 expressing muscle-derived stem cells from 15% to 80% [5]. Since we have used MDPCs that highly express Sca-1

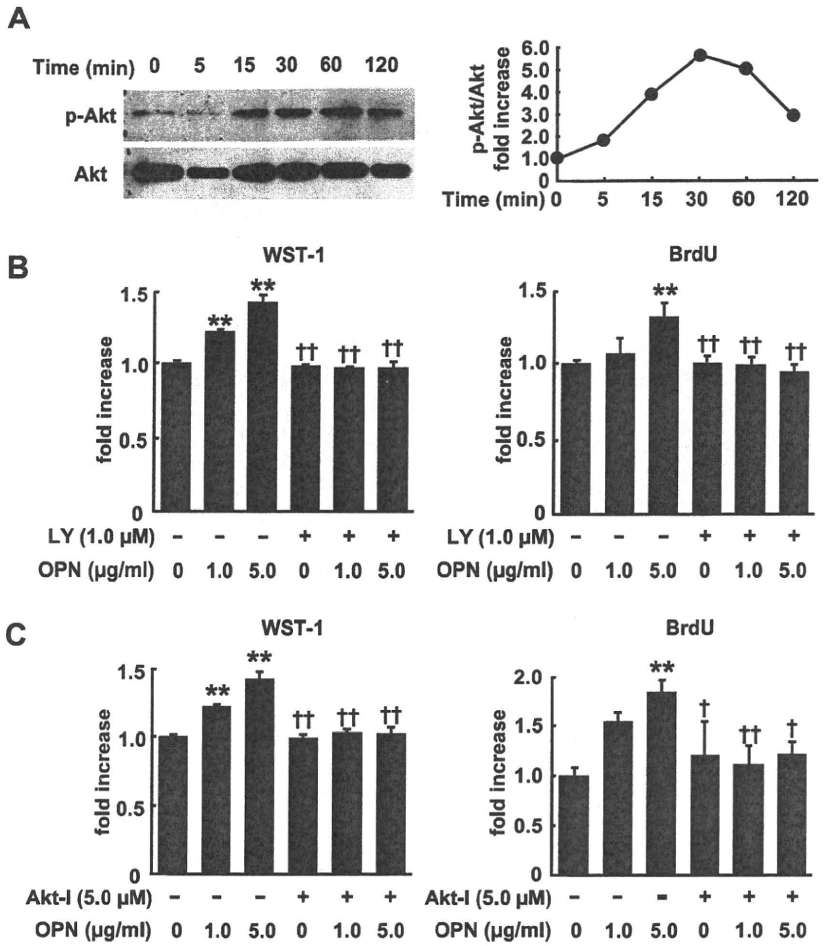

Fig. 3. OPN stimulates proliferation of MDPCs through the PI3K/Akt signaling pathway. (A) MDPCs were treated with 5.0 μg/ml OPN for various time periods. Cell extracts were subjected to Western blotting (left panel) using an anti-phospho-specific Akt antibody (p-Akt, upper panel) or an anti-Akt antibody (Akt, lower panel). Right graph shows the time course of relative phosphorylation of Akt during OPN treatment. The experiment shown represents one of three independent trials that gave nearly identical results. (B,C) Cell proliferation activity was assessed by use of the WST-1 and BrdU ELISA assay systems. Cell proliferation and DNA synthesis of MDPCs induced by OPN were inhibited by pretreatment with LY294004, a PI3K inhibitor (B), or Akt inhibitor (C). Values are means ± SEM. LY, LY294002; Akt-I, Akt inhibitor. $^{**}P < 0.01$ vs control; $^{\dagger}P < 0.05$, $^{\dagger\dagger}P < 0.01$ vs 5.0 μg/ml OPN.

(FACS analysis, 84.0 ± 2.6%) [6], the discrepant result between our study and Sarig et al. [5] regarding the effect of LIF might be due to the population of Sca-1 expressing cells. We also found that OPN expression was enhanced by bFGF but not EGF and LIF in MDPCs, and that OPN promotes MDPC proliferation. These findings suggest that OPN contributes to bFGF-induced MDPC proliferation.

OPN has a protease-hypersensitive site that separates the integrin- and CD44-binding domains and exerts its effects by interacting with various integrins and CD44 receptors [14]. We have shown that CD29 (also known as β1 integrin) and CD44 are expressed on MDPCs [6]. OPN has been shown to activate the PI3K/Akt signaling pathway through αvβ3 integrin- and CD44-mediated pathways [21,22]. Furthermore, CD44 has been demonstrated to cooperate with β1 integrin to bind OPN [23]. Therefore, our findings suggest that CD44 and β1 integrin may mediate OPN-induced activation of the PI3K/Akt signaling pathway and allow the proliferative growth of MDPCs.

Extensive research using OPN-knockdown by siRNA and OPN-null mutant mice has demonstrated that OPN promotes the growth or survival of tumor cells [14,24–27]. Similar to the effect of OPN on tumor cells, we showed a proliferative effect of OPN on MDPCs in the present study. We also demonstrated that OPN-treated MDPCs retained the ability to differentiate into vascular cells. OPN expression has been revealed to be up-regulated in regenerating skeletal muscle after injury [28]. A study using OPN-null mutant mice also demonstrated that OPN was required for efficient angiogenesis in ectopically implanted bone discs in skeletal muscle [29]. Taken together with our findings, these data suggest that OPN is involved in the proliferation of MDPCs and angiogenesis by MDPCs in skeletal muscle. However, in primitive hematopoietic stem cells (HSCs) OPN has been reported to be a critical component of the HSC niche within the bone marrow microenvironment, and to work as a negative regulator of HSC proliferation [30,31]. The reason why OPN has opposite

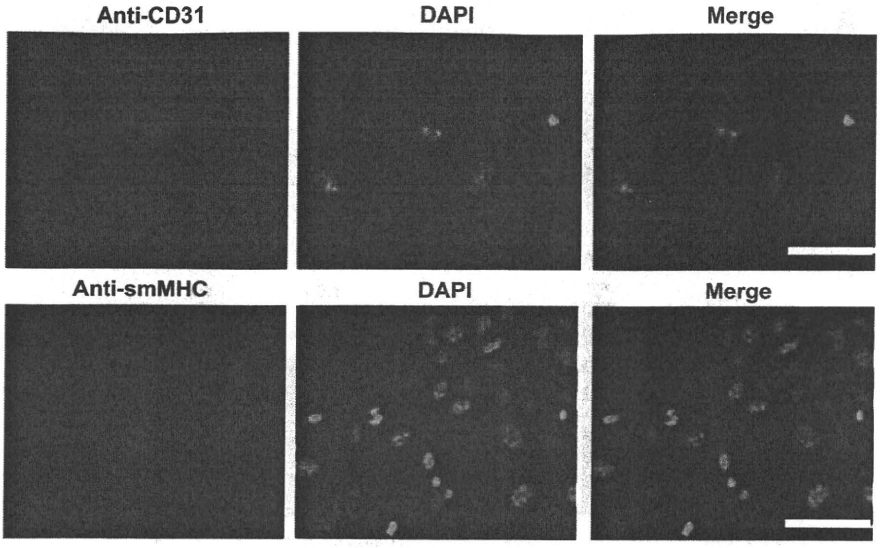

Fig. 4. MDPCs maintain a capacity of differentiation into cardiovascular lineages after treatment with OPN. Immunostaining was performed using an anti-CD31 antibody or an anti-smMHC antibody. MDPCs treated with OPN were differentiated into CD31 positive endothelial (red) or smMHC positive smooth muscle (red) cells by VEGF or PDGF, respectively. Nuclei were stained by DAPI (blue). Bar indicates 50 μm.

effects on HSC and MDPC proliferation is unclear. HSCs have been shown to express several integrins and various isoforms of CD44 [32]. Except for the expression of CD44 and β1 integrin on MDPCs [6], it remains to be determined whether isoforms of CD44 and other integrins are expressed on MDPCs. Since the different effects that OPN elicits can be attributed to its multiple receptors, binding sites, and various forms [33], the expression pattern of integrins and CD44 isoforms in MDPCs may differ from that in HSCs.

In conclusion, we identified OPN as a secreted molecule in MDPCs by using SAGE and SST. Recombinant OPN had a proliferative effect on MDPCs with or without various growth factors, and PI3K/Akt signaling was involved in the effect. Furthermore, MDPCs treated with OPN had an enhanced proliferative potential and maintained their potency to differentiate into vascular lineages. Thus, OPN may be one of the candidate autocrine/paracrine molecules that could be applied in a therapeutic intervention using MDPCs to treat patients with vascular diseases.

Acknowledgments

We are grateful to Ms. A. Kosugi, Ms. M. Nishikawa, and Mr. M. Kuramoto for their skillful technical assistance. This work was supported by Grants-in-Aid from the Ministry of Education, Culture, Sports, Science and Technology of Japan, and by Grants-in-Aid from the Ministry of Health, Labor, and Welfare of Japan, Japan Association for the Advancement of Medical Equipment, Takeda Science Foundation, Novartis Research Award on Molecular and Cellular Cardiology, Kanae Foundation for Life & Socio-Medical Science, Suzuken Memorial Foundation, and Mochida Memorial Foundation.

References

[1] Z. Qu-Petersen, B. Deasy, R. Jankowski, M. Ikezawa, J. Cummins, R. Pruchnic, J. Mytinger, B. Cao, C. Gates, A. Wernig, J. Huard, Identification of a novel population of muscle stem cells in mice: potential for muscle regeneration, J. Cell Biol. 157 (2002) 851–864.

[2] H. Oshima, T.R. Payne, K.L. Urish, T. Sakai, Y. Ling, B. Gharaibeh, K. Tobita, B.B. Keller, J.H. Cummins, J. Huard, Differential myocardial infarct repair with muscle stem cells compared to myoblasts, Mol. Ther. 12 (2005) 1130–1141.

[3] T.R. Payne, H. Oshima, T. Sakai, Y. Ling, B. Gharaibeh, J. Cummins, J. Huard, Regeneration of dystrophin-expressing myocytes in the mdx heart by skeletal muscle stem cells, Gene Ther. 12 (2005) 1264–1274.

[4] T. Tamaki, A. Akatsuka, K. Ando, Y. Nakamura, H. Matsuzawa, T. Hotta, R.R. Roy, V.R. Edgerton, Identification of myogenic-endothelial progenitor cells in the interstitial spaces of skeletal muscle, J. Cell Biol. 157 (2002) 571–577.

[5] R. Sarig, Z. Baruchi, O. Fuchs, U. Nudel, D. Yaffe, Regeneration and transdifferentiation potential of muscle-derived stem cells propagated as myospheres, Stem Cells 24 (2006) 1769–1778.

[6] T. Nomura, E. Ashihara, K. Tateishi, S. Asada, T. Ueyama, T. Takahashi, H. Matsubara, H. Oh, Skeletal myosphere-derived progenitor cell transplantation promotes neovascularization in δ-sarcoglycan knockdown cardiomyopathy, Biochem. Biophys. Res. Commun. 352 (2007) 668–674.

[7] P. Taupin, J. Ray, W.H. Fischer, S.T. Suhr, K. Hakansson, A. Grubb, F.H. Gage, FGF-2-responsive neural stem cell proliferation requires CCg, a novel autocrine/paracrine cofactor, Neuron 28 (2000) 385–397.

[8] Y. Arsenijevic, S. Weiss, B. Schneider, P. Aebischer, Insulin-like growth factor-I is necessary for neural stem cell proliferation and demonstrates distinct actions of epidermal growth factor and fibroblast growth factor-2, J. Neurosci. 21 (2001) 7194–7202.

[9] H. Toda, M. Tsuji, I. Nakano, K. Kobuke, T. Hayashi, H. Kasahara, J. Takahashi, A. Mizoguchi, T. Houtani, T. Sugimoto, N. Hashimoto, T.D. Palmer, T. Honjo, K. Tashiro, Stem cell-derived neural

stem/progenitor cell supporting factor is an autocrine/paracrine survival factor for adult neural stem/progenitor cells, J. Biol. Chem. 278 (2003) 35491–35500.
[10] T. Nakamura, P. Ruiz-Lozano, V. Lindner, D. Yabe, M. Taniwaki, Y. Furukawa, K. Kobuke, K. Tashiro, Z. Lu, N.L. Andon, R. Schaub, A. Matsumori, S. Sasayama, K.R. Chien, T. Honjo, DANCE, a novel secreted RGD protein expressed in developing, atherosclerotic, and balloon-injured arteries, J. Biol. Chem. 274 (1999) 22476–22483.
[11] T. Kojima, T. Kitamura, A signal sequence trap based on a constitutively active cytokine receptor, Nat. Biotechnol. 17 (1999) 487–490.
[12] V.E. Velculescu, B. Vogelstein, K.W. Kinzler, Analysing uncharted transcriptomes with SAGE, Trends Genet. 16 (2000) 423–425.
[13] S.B. Rodan, G. Wesolowski, K. Yoon, G.A. Rodan, Opposing effects of fibroblast growth factor and pertussis toxin on alkaline phosphatase, osteopontin, osteocalcin, and type I collagen mRNA levels in ROS 17/2.8 cells, J. Biol. Chem. 264 (1989) 19934–19941.
[14] H. Rangaswami, A. Bulbule, G.C. Kundu, Osteopontin: role in cell signaling and cancer progression, Trends Cell Biol. 16 (2006) 79–87.
[15] K. Tateishi, E. Ashihara, S. Honsho, N. Takehara, T. Nomura, T. Takahashi, T. Ueyama, M. Yamagishi, H. Yaku, H. Matsubara, H. Oh, Human cardiac stem cells exhibit mesenchymal features and are maintained through Akt/GSK-3β signaling, Biochem. Biophys. Res. Commun. 352 (2007) 635–641.
[16] D.N. Haylock, S.K. Nilsson, Osteopontin: a bridge between bone and blood, Br. J. Haematol. 134 (2006) 467–474.
[17] S. Temple, A. Alvarez-Buylla, Stem cells in the adult mammalian central nervous system, Curr. Opin. Neurobiol. 9 (1999) 135–141.
[18] A. Gritti, E.A. Parati, L. Cova, P. Frolichsthal, R. Galli, E. Wanke, L. Faravelli, D.J. Morassutti, F. Roisen, D.D. Nickel, A.L. Vescovi, Multipotential stem cells from the adult mouse brain proliferate and self-renew in response to basic fibroblast growth factor, J. Neurosci. 16 (1996) 1091–1100.
[19] B.A. Reynolds, S. Weiss, Clonal and population analyses demonstrate that an EGF-responsive mammalian embryonic CNS precursor is a stem cell, Dev. Biol. 175 (1996) 1–13.
[20] E. Messina, L. De Angelis, G. Frati, S. Morrone, S. Chimenti, F. Fiordaliso, M. Salio, M. Battaglia, M.V. Latronico, M. Coletta, E. Vivarelli, L. Frati, G. Cossu, A. Giacomello, Isolation and expansion of adult cardiac stem cells from human and murine heart, Circ. Res. 95 (2004) 911–921.
[21] Y.H. Lin, H.F. Yang-Yen, The osteopontin-CD44 survival signal involves activation of the phosphatidylinositol 3-kinase/Akt signaling pathway, J. Biol. Chem. 276 (2001) 46024–46030.
[22] R. Das, G.H. Mahabeleshwar, G.C. Kundu, Osteopontin stimulates cell motility and nuclear factor κB-mediated secretion of urokinase type plasminogen activator through phosphatidylinositol 3-kinase/Akt signaling pathways in breast cancer cells, J. Biol. Chem. 278 (2003) 28593–28606.
[23] Y.U. Katagiri, J. Sleeman, H. Fujii, P. Herrlich, H. Hotta, K. Tanaka, S. Chikuma, H. Yagita, K. Okumura, M. Murakami, I. Saiki, A.F. Chambers, T. Uede, CD44 variants but not CD44s cooperate with β1-containing integrins to permit cells to bind to osteopontin independently of arginine-glycine-aspartic acid, thereby stimulating cell motility and chemotaxis, Cancer Res. 59 (1999) 219–226.
[24] H.C. Crawford, L.M. Matrisian, L. Liaw, Distinct roles of osteopontin in host defense activity and tumor survival during squamous cell carcinoma progression in vivo, Cancer Res. 58 (1998) 5206–5215.
[25] Y. Wu, D.T. Denhardt, S.R. Rittling, Osteopontin is required for full expression of the transformed phenotype by the ras oncogene, Br. J. Cancer 83 (2000) 156–163.
[26] S.R. Rittling, A.F. Chambers, Role of osteopontin in tumour progression, Br. J. Cancer 90 (2004) 1877–1881.
[27] D. Denhardt, Osteopontin expression correlates with melanoma invasion, J. Invest. Dermatol. 124 (2005) xvi–xviii.
[28] A. Hirata, S. Masuda, T. Tamura, K. Kai, K. Ojima, A. Fukase, K. Motoyoshi, K. Kamakura, Y. Miyagoe-Suzuki, S. Takeda, Expression profiling of cytokines and related genes in regenerating skeletal muscle after cardiotoxin injection: a role for osteopontin, Am. J. Pathol. 163 (2003) 203–215.
[29] Y. Asou, S.R. Rittling, H. Yoshitake, K. Tsuji, K. Shinomiya, A. Nifuji, D.T. Denhardt, M. Noda, Osteopontin facilitates angiogenesis, accumulation of osteoclasts, and resorption in ectopic bone, Endocrinology 142 (2001) 1325–1332.
[30] S.K. Nilsson, H.M. Johnston, G.A. Whitty, B. Williams, R.J. Webb, D.T. Denhardt, I. Bertoncello, L.J. Bendall, P.J. Simmons, D.N. Haylock, Osteopontin, a key component of the hematopoietic stem cell niche and regulator of primitive hematopoietic progenitor cells, Blood 106 (2005) 1232–1239.
[31] S. Stier, Y. Ko, R. Forkert, C. Lutz, T. Neuhaus, E. Grunewald, T. Cheng, D. Dombkowski, L.M. Calvi, S.R. Rittling, D.T. Scadden, Osteopontin is a hematopoietic stem cell niche component that negatively regulates stem cell pool size, J. Exp. Med. 201 (2005) 1781–1791.
[32] P.J. Simmons, J.P. Levesque, A.C. Zannettino, Adhesion molecules in haemopoiesis, Baillieres Clin. Haematol. 10 (1997) 485–505.
[33] D.T. Denhardt, X. Guo, Osteopontin: a protein with diverse functions, FASEB J. 7 (1993) 1475–1482.

Clonally amplified cardiac stem cells are regulated by Sca-1 signaling for efficient cardiovascular regeneration

Kento Tateishi[1,2], Eishi Ashihara[1], Naofumi Takehara[1], Tetsuya Nomura[1,2], Shoken Honsho[2], Takuo Nakagami[2,3], Shigehiro Morikawa[4], Tomosaburo Takahashi[1,2], Tomomi Ueyama[1], Hiroaki Matsubara[1,2,*] and Hidemasa Oh[1,*]

[1]Department of Experimental Therapeutics, Translational Research Center, Kyoto University Hospital, Kyoto 606-8507, Japan
[2]Department of Cardiovascular Medicine, [3]Departments of Pathology and Cell Regulation, Kyoto Prefectural University of Medicine, Kyoto 602-8566, Japan
[4]Molecular Neuroscience Research Center, Shiga University of Medical Science, Shiga 520-2192, Japan
*Authors for correspondence (e-mail: matsubah@koto.kpu-m.ac.jp; hidemasa@kuhp.kyoto-u.ac.jp)

Accepted 25 March 2007
Journal of Cell Science 120, 1791-1800 Published by The Company of Biologists 2007
doi:10.1242/jcs.006122

Summary

Recent studies have shown that cardiac stem cells (CSCs) from the adult mammalian heart can give rise to functional cardiomyocytes; however, the definite surface markers to identify a definitive single entity of CSCs and the molecular mechanisms regulating their growth are so far unknown. Here, we demonstrate a single-cell deposition analysis to isolate individually selected CSCs from adult murine hearts and investigate the signals required for their proliferation and survival. Clonally proliferated CSCs express stem cell antigen-1 (Sca-1) with embryonic stem (ES) cell-like and mesenchymal cell-like characteristics and are associated with telomerase reverse transcriptase (TERT). Using a transgene that expresses a GFP reporter under the control of the TERT promoter, we demonstrated that $TERT^{GFP}$-positive fractions from the heart were enriched for cells expressing Sca-1. Knockdown of Sca-1 transcripts in CSCs led to retarded ex vivo expansion and apoptosis through Akt inactivation. We also show that ongoing CSC proliferation and survival after direct cell-grafting into ischemic myocardium require Sca-1 to upregulate the secreted paracrine effectors that augment neoangiogenesis and limit cardiac apoptosis. Thus, Sca-1 might be an essential component to promote CSC proliferation and survival to directly facilitate early engraftment, and might indirectly exert the effects on late cardiovascular differentiation after CSC transplantation.

Key words: Cardiac stem cells, Proliferation, Regeneration, Stem cell antigen-1, Survival, Telomerase

Introduction

The adult mammalian heart harbors a population of mitotically competent cardiac stem cells (CSCs) that can be isolated by using FACS to recognize the cells expressing surface antigens KIT and stem cell antigen-1 (Sca-1) or by targeting a reporter gene driven by the promoter for islet-1, a LIM-homeodomain transcription factor (Beltrami et al., 2003; Laugwitz et al., 2005; Matsuura et al., 2004; Moretti et al., 2006; Oh et al., 2003; Pfister et al., 2005). These cells express essential cardiac transcriptional factors but do not express more mature markers of structural genes; however, the exact contribution of cell fusion in the process of adopting cardiac muscle phenotype after cell transfer into ischemic myocardium remains controversial (Beltrami et al., 2003; Oh et al., 2003). Within the adult heart, CSCs often reside in cardiac niches with supporting cells that provide a specialized environment to replenish and maintain a balance of survival, proliferation and self-renewal of CSCs through symmetric or asymmetric division in order to replace the mature cells that are lost during injury or turnover (Urbanek et al., 2006).

The general lack of definitive molecular markers to identify cardiac stem cells raises the fundamental question of whether these cardiac stem cells are derived from a single entity. CSCs in the mammalian heart share several cell-surface markers with hematopoietic and endothelial progenitor cells (Linke et al., 2005; Messina et al., 2004; Urbanek et al., 2003). Although the hierarchies of hematopoietic stem cells have been well characterized, evidence supporting the role of bone marrow-derived *Lin⁻-Kit⁺* cells in cardiac-lineage induction has been controversial (Kawada et al., 2004; Murry et al., 2004; Orlic et al., 2001). Recent reports have demonstrated that genetic disruption of *Kit* in mice mainly affects marrow-derived hematopoietic and endothelial cell development for cardiac repair, that could be rescued by bone marrow replacement with wild-type cells, through the failure of progenitor-cell mobilization from marrow and reduced release of cytokines and chemokines that may participate in the cardioprotective paracrine signaling (Ayach et al., 2006; Fazel et al., 2006). These studies do not exclude the possible functional role of KIT in resident CSCs as the principal mediator in the regenerating process during cardiac injury, but suggest that defining CSCs using specific cell-surface markers may not be optimal to address the identity of these cells, as indicated by their partially overlapping expression in human hearts (Urbanek et al., 2005b).

Decline of CSC function may be a major cause of the decrease in regenerative capacity in aging and disease (Rota et al., 2006). Although some of the growth factors involved in *Kit*$^{+}$ CSC proliferation and survival have been identified, factors regulating *Kit*$^{-}$ CSCs have yet to be defined (Gude et al., 2006; Limana et al., 2005; Urbanek et al., 2005a). In this study, we sought to identify single proliferative cells from the adult heart without progenitor selection using particular surface markers. Using this unbiased approach, we have established clonal CSC lines and demonstrated that the majority of the telomerase-active progenitor-cell colonies expressed Sca-1 and showed mesenchymal-cell-like character. We also show that targeting the Sca-1 transcripts in CSCs used for cell grafting leads to failure of their ability to prevent cardiac remodeling after myocardial infarction. The antiapoptotic and angiogenetic paracrine activities of intrinsic Sca-1 signaling in CSCs promote direct CSC proliferation and survival, and contribute to neovascularization in the host myocardium for efficient cardiovascular regeneration.

Results

Clonal isolation of cardiac stem cells in the adult heart

To identify the single entity of CSCs in the adult heart, we employed an unbiased approach using a single-cell clonogenic isolation technique to isolate a proliferative cell population. Singly dissociated GFP-labelled transgenic cells derived from the hearts of GFP transgenic mice were plated at a density of one cell per well in serum-free medium (Fig. 1A,B). Altogether, 11,520 single cells were deposited, and from 9541 single cells determined by inspection on day 1 to be present as one individual cell per well, a total of 11 clones arose within 7 days. Eight out 11 clones failed to grow in serum-free medium after 7 days in culture, and 3 clones (~0.03%) could proliferate to form spherical clusters and were continuously expanded after 14 days (Fig. 1C). The three independent colonies were re-dissociated and re-plated in low-serum for expansion, and individual CSC colonies were used for the following experiments to characterize clonal CSCs.

Characterization of clonally amplified CSCs

Immunophenotyping revealed that the clonal CSCs strongly expressed Sca-1, which is used as a marker to identify cardiac progenitor cells from the adult heart (Matsuura et al., 2004; Oh et al., 2003), whereas KIT-positive cells were rarely detected (Fazel et al., 2006; Gude et al., 2006; Pfister et al., 2005) (Fig. 1D). Notably, CSCs did not express the hematopoietic and endothelial progenitor-cell-specific surface antigens CD45, CD34 and CD31, but did express the typical mesenchymal stem-cell surface antigens CD90, CD105, CD29, CD44, CD106, CD73 and CD13 (Pittenger and Martin, 2004). The three individual CSCs exhibited an identical immunophenotyping for the surface marker analysis. The cell membrane antigens Sca-1, KIT, CD45, and CD34 were not destroyed by collagenase treatment as tested in bone marrow (data not shown).

Gene expression was then examined in CSC clones using reverse transcriptase (RT)-PCR (Fig. 1E). Three individual colonies were analyzed and most of the clones expressed Bcrp1, polycomb group protein Bmi1 and also telomerase reverse transcriptase (TERT), which has been reported to be absent in cardiac fibroblasts (Leri et al., 2001). Although Nanog was detectable in all of the colonies examined, none of the colonies – unlike embryonic stem (ES) cells – were positive for OCT4 or UTF1. Some but not all of the colonies expressed HNF3β, brachyury and SOX2, which are endodermal, mesodermal and ectodermal precursor markers, respectively. These results distinguished clonal CSCs from mouse fibroblasts, which are negative for all of the ES cell markers described above (Takahashi and Yamanaka, 2006). In addition, all of the colonies analyzed expressed nestin, a marker of immature neural progenitor cells (Joannides et al., 2004).

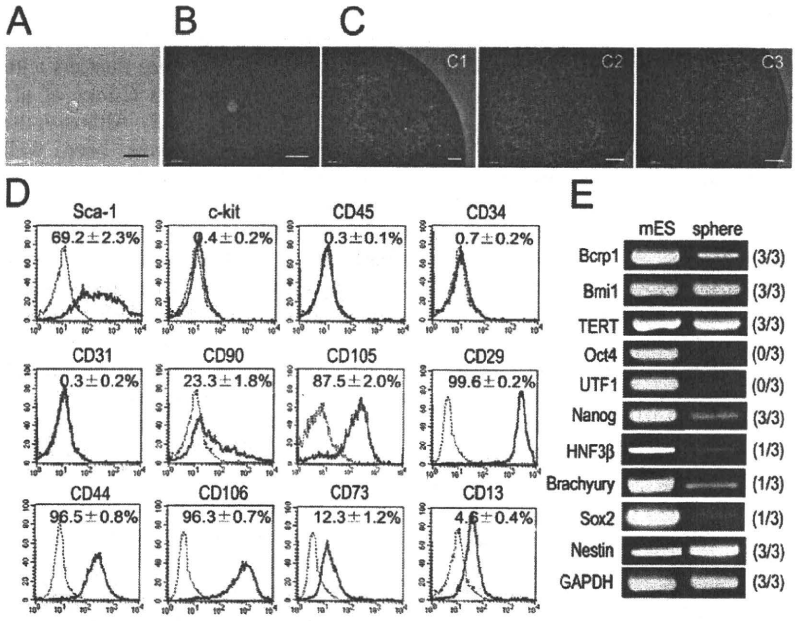

Fig. 1. Clonal isolation and characterization of stem cells in the adult heart. (A,B) Single-cell deposition analysis was performed by the limiting dilution technique. At day 1 of the culture period, wells were inspected for the presence of single cells by phase contrast (A) and GFP fluorescence (B). (C) Colony formation from single cells in 96-well plates at 14 days of culture in serum-free medium. Three-independent colonies derived from single cells are shown. (D) FACS analysis of CSCs. Black line, control IgG; red line, corresponding antibody. Data are representative of three independent clonal CSCs. (E) RT-PCR for CSC clones. The numbers on the right indicate the number of individual colonies that expressed the corresponding genes out of the colonies examined. mES, mouse ES cells used as positive control. Data are representative of three independent clonal CSCs. Bars, 20 μm in A,B; 500 μm in C.

TERT-expressing cells in postnatal heart are associated with Sca-1 expression

TERT has been identified as a key factor controlling telomerase activity, telomere length, and cell growth (Blackburn, 2001). We measured the telomerase activity in clonal CSCs. The three individual CSCs displayed significantly elevated telomerase activity (Fig. 2A). To directly characterize TERT-expressing cells in the adult heart, we engineered transgenic mice expressing enhanced green fluorescent protein (EGFP) under the control of the mouse *Tert* promoter (Fig. 2B). We identified two transgenic founders by genomic DNA screening and established two independent lines (Fig. 2C). In order to examine the efficacy of mouse *Tert* promoter in the heart in vivo, cells isolated from transgenic hearts were sorted by EGFP signal and the EGFP-positive cells were found to be TERT-expressing cells, which were not detectable in EGFP$^-$ populations (Fig. 2D). As expected from high telomerase activities of clonal CSCs shown in Fig. 2A, three individual CSC clones showed TERT expression (Fig. 2D). To further characterize the TERT-positive cells in the heart, FACS analysis was performed. FACS of the cells prepared from the heart of adult mice expressing TERT-EGFP indicated that TERT^{GFP}-positive cells constitute a population that is positive for Sca-1 but rarely expressing detectable levels of c-kit, CD45, CD34, or CD31 (Fig. 2E).

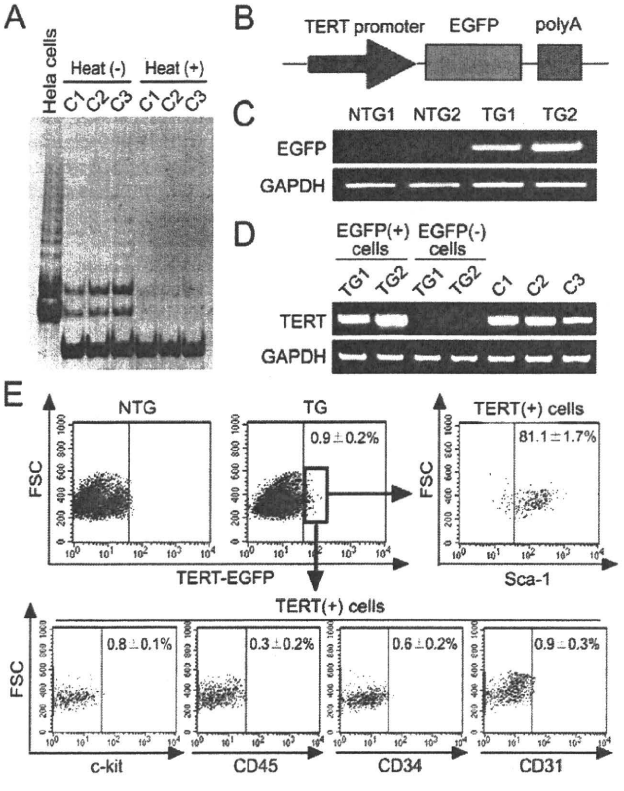

Fig. 2. TERT-expressing cells in adult heart are associated with Sca-1 expression. (A) Telomerase activity was measured by the TRAP assay in three independent clonal-CSCs. The cells were treated with or without heat and used as templates. Hela cells were used as positive controls. (B) Construction of EGFP transgene under the control of the TERT promoter. (C) PCR of genomic DNA from 2 independent TERT-EGFP transgenic lines and respective NTG littermate controls. (D) The expression of TERT on EGFP-positive and EGFP-negative cells sorted from TERT-EGFP transgenic hearts is shown by RT-PCR. The TERT expression was detectable in all three independent clonal CSCs shown in Fig. 1C. (E) FACS analysis of the primary EGFP-positive cells isolated from TERT-EGFP mice (TG). Expression of Sca-1, KIT, CD45, CD34, and CD31 in EGFP-positive cells was examined. Cells from NTG littermates were used as negative control. Data are representative of six independent experiments.

Generation of Sca-1 knockdown (KD) mice

To functionally characterize clonal CSCs, majority of which could be marked by Sca-1 expression, we generated Sca-1 KD mice in which double-stranded (ds)-Sca-1 RNA was expressed under the control of an RNA polymerase II promoter (Fig. 3A) (Shinagawa and Ishii, 2003). The vector pDECAP-Sca-1 expressing ds-Sca-1 RNA with a small loop for transcript pausing and full-length Sca-1 were co-transfected into HEK 293 cells at various concentrations, and the reduction in Sca-1 expression was examined by both RT-PCR and FACS (Fig. 3B,C). Two lines of Sca-1 KD mice were obtained, in which endogenous Sca-1 protein levels (Fig. 3D) in the heart were apparently reduced.

Targeting Sca-1 transcripts affects proliferation and survival but not differentiation of CSCs

To test the function of Sca-1 in CSC development, we examined the ability to clonally proliferate in vitro of single cells from the adult heart of Sca-1 KD and non-transgenic (NTG) littermate mice using a single-cell deposition analysis. This revealed that the percentage of colony-forming cells from Sca-1 KD hearts was significantly lower than that from NTG hearts (Sca-1 KD ~0.007% vs NTG ~0.03%, Fig. 3E). We isolated 11 clones from NTG hearts and four clones from Sca-1 KD hearts, of which eight NTG- and two Sca-1 KD-clones exhibited features of mesenchymal phenotype (data not shown), showed Nanog and Bcrp1 expression by RT-PCR, and could proliferate for more than 14 days (Fig. 3F). Of the clones obtained, four clones expressed brachyury, which is a primitive streak marker (Gadue et al., 2006). Sca-1 expression in CSCs isolated from Sca-1 KD mice was markedly inhibited compared with NTG controls (Fig. 3G). Therefore, we investigated whether Sca-1 expression affects the replicative growth of clonal CSCs in independent cell-culture (Fig. 3H). As shown in Fig. 3I, Sca-1 KD CSCs showed significantly impaired growth kinetics compared with those of NTG CSCs. We determined the molecular mechanisms by which Sca-1 KD mice showed retarded CSC growth. As shown in Fig. 3J, BrdU incorporation and phosphorylation of histone H3 were clearly reduced in the Sca-1 KD CSCs compared with NTG controls, whereas p53 expression levels were significantly increased in the Sca-1 KD CSCs. Telomerase activities were also significantly impaired in the Sca-1 KD CSCs (Fig. 3K).

Of the CSC clones isolated, clones 2, 3 and 6 from NTG and clone 1 from Sca-1 KD mice, all of which expressed brachyury, were chosen for subsequent series of experiments. We asked whether the decrease in clonal CSC growth mediated by Sca-1 KD is associated with an increase in apoptosis. CSCs were isolated from the hearts of NTG and Sca-1 KD mice and were incubated with 100 and 200 μM H_2O_2 for 18 hours, and the surviving cells were analyzed by TUNEL staining. As shown

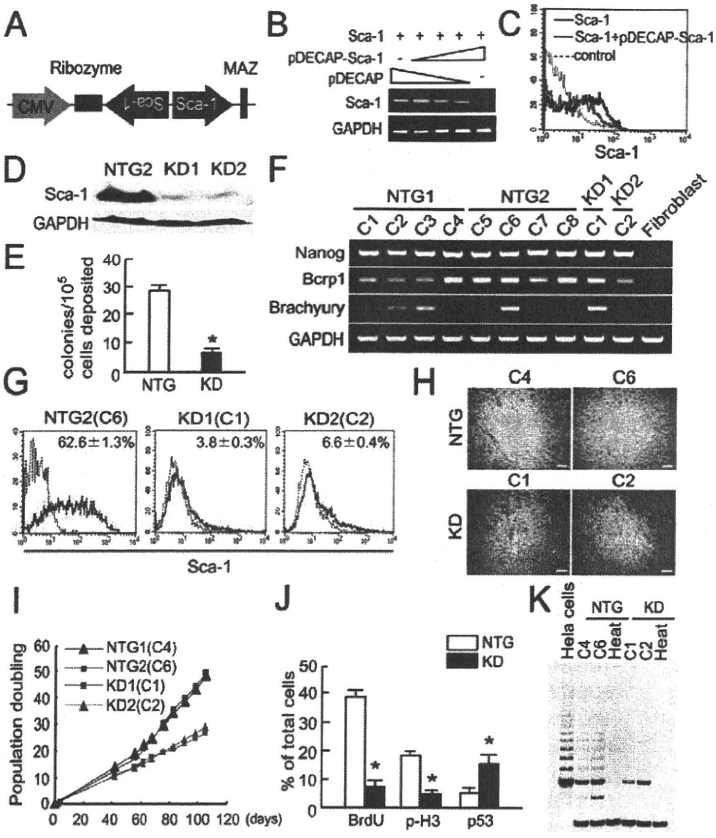

Fig. 3. Generation of Sca-1 KD mice. (A) Construction of the pDECAP-Sca-1 vector. (B,C) Decrease in exogenous Sca-1 expression induced by pDECAP-Sca-1 as shown by RT-PCR (B) and FACS (C) in HEK 293 cells. The total amount (8 μg) of plasmids co-transfected was the same in each experiment (n=3). (D) Decrease in Sca-1 protein levels in the hearts from two independent Sca-1 KD lines. (E) The frequency of CSC colonies from NTG- and Sca-1 KD hearts is shown. Data are expressed as the mean number of colonies formed per 10^5 single cells deposited ± s.e. (n=4). *P<0.01 vs NTG. (F) RT-PCR for embryonic and mesodermal precursor markers. Cardiac fibroblasts were used as negative control. (G) Decrease in Sca-1 expression from two independent Sca-1 KD CSCs clones. Black line, control IgG; red line, Sca-1. (H) Phase-contrast images of respective CSC clones at 14 days of culture in serum-free medium. Bars, 500 μm. (I) Growth kinetics of two independent clonal CSCs isolated from NTG (black lines, C4 and C6) and Sca-1 KD (red lines, C1 and C2) mice. (J) BrdU incorporation, phosphorylated histone-H3 (p-H3) and p53 expression from five independent experiments are shown. *P<0.01 vs NTG. (K) Loss of telomerase activity in the clonal CSCs (C1 and C2) isolated from two independent lines of Sca-1 KD mice.

in Fig. 4A, H_2O_2 induced apoptosis in a dose-dependent manner, and the extent of apoptosis was significantly higher in CSCs isolated from Sca-1 KD hearts than that in NTG-CSCs.

Activation of EGF and bFGF signaling in endothelial cells leads to the phosphorylation of a number of downstream effectors, including Akt and MAPKs (Sulpice et al., 2002). To test the role of these kinases in Sca-1-mediated CSC growth, the activation of Akt and MAPKs in response to EGF and bFGF was examined (Fig. 4B). Incubation of CSCs with EGF and bFGF resulted in a rapid enhancement of Akt, ERK1/2, and JNK1/2, but not in phosphorylation of p38. Although activation of Akt could be abolished by inhibition of Sca-1 transcripts, phosphorylation of three MAPKs was unaffected. These results raise the issue of whether Sca-1-mediated signaling regulates CSC differentiation in vitro. The potential of CSCs to give rise to cardiovascular lineages was not affected by targeting Sca-1 transcripts – as shown by immunostaining (Fig. 5A) and by RT-PCR to assess gene profiles typical of cardiac muscle, smooth muscle and endothelial cell differentiation after specific inductions for 14 days (Fig. 5B),

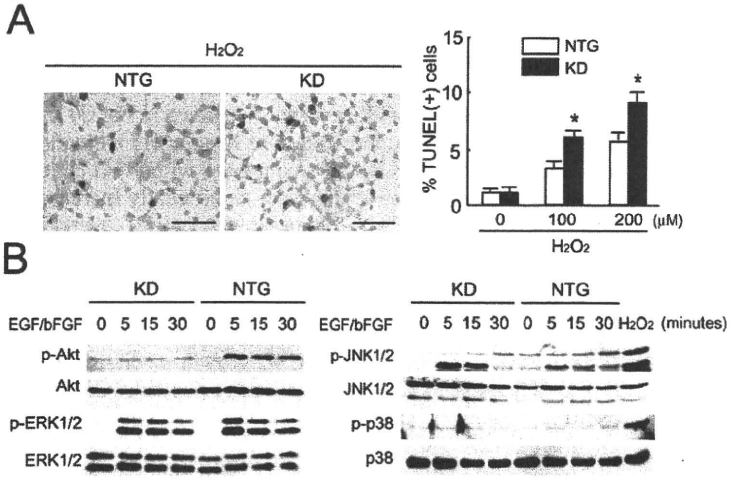

Fig. 4. Sca-1-mediated signaling activates Akt to support CSC proliferation and survival.
(A) Representative photographs of TUNEL assay obtained from NTG- or Sca-1 KD-derived CSCs treated with 200 μM H_2O_2 for 18 hours. The numbers of apoptotic cells (brown nuclei) in NTG (C6)- or Sca-1 KD-CSCs (C1) are shown (n=8). *P<0.01 versus NTG. (B) Loss of Sca-1 diminished EGF and bFGF-induced Akt activation in CSCs. CSCs treated with 200 μm H_2O_2 for 15 minutes were used as positive controls. Bars, 50 μm in A.

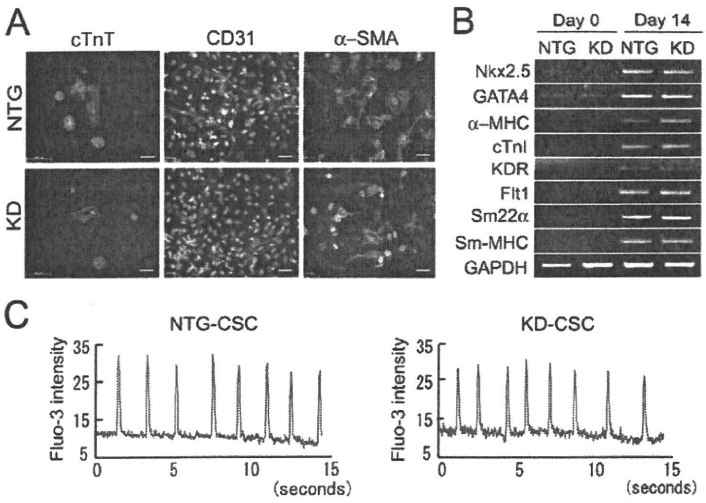

Fig. 5. Loss of Sca-1 transcripts does not affect the differentiation potential of clonal CSCs.
(A) Differentiation of NTG-derived or Sca-1 KD-derived clonal CSCs. Cardiac muscle cell (cardiac troponin-T), endothelial cell (CD31) and vascular smooth muscle cell (α-SMA) differentiation were 1.24±0.3%, 12.4±1.8% and 31.9±2.5%, respectively, for NTG-CSCs (C2, C3 and C6, respectively), and 1.23±0.3%, 12.1±2.1% and 32.2±4.7%, respectively, for Sca-1 KD-CSCs (C1). Nuclei are stained by DAPI (blue). Bars, 20 μm in A. (B) RT-PCR showed that the differentiation potential into the three different lineages were similar for both types of CSCs (n=3).
(C) Representative Ca^{2+} transient in beating cardiomyocytes. Clone 2, 3 and 6 from NTG and clone 1 from Sca-1 KD mice, all expressed brachyury at baseline, were used for analysis. Intensities were corrected by background amplitude and expressed as arbitrary units (n=3).

and a study investigating the Ca^{2+} transient in beating cardiomyocytes (Fig. 5C).

Loss of Sca-1 transcripts in CSCs fails to improve cardiac function due to diminished donor-cell proliferation, survival and engraftment after cell transplantation

The data described above support the hypothesis that loss of Sca-1 results in a retarded regenerative capacity of CSCs in vivo. To further examine this possibility, we performed cell transfer experiments into ischemic myocardium. 5×10^5 CSCs that had been clonally isolated and expanded from the hearts of Sca-1 KD (C1) and NTG (C6) mice were transplanted into wild-type (WT) mice 1 hour after myocardial infarction. Cardiac MRI was performed 4 weeks after cell grafting and showed that transplantation of Sca-1-KD CSCs resulted in significantly larger left ventricular volume and an increased infarct rate as compared with NTG-CSC implantation (Fig. 6A,B).

We examined the in-vivo effects of Sca-1-mediated CSC regulation we observed in vitro. At day 3 after CSC transplantation into ischemic myocardium, Sca-1 KD CSCs showed significantly fewer engraftments than NTG-CSCs, as verified by measurement of *lacZ* activity (Fig. 7A). This observation was confirmed by the lower Ki67 expression in Sca-1 KD CSCs, indicating that the proliferative potential was significantly impaired in Sca-1 KD CSCs (Fig. 7A). To assess whether Sca-1-mediated control of CSC survival may also be applied to the process of donor-cell engraftment, we analyzed the viability of grafted CSCs, labeled by β-galactosidase (β-gal) staining, on day 3 after the cell grafting. As shown in Fig. 7B, grafted Sca-1 KD CSCs in the ischemic myocardium resulted in more apoptotic cells than NTG-CSCs, suggesting that the transplanted Sca-1 KD CSCs were also susceptible to cell death in vivo.

To further test whether these effects of Sca-1 during the early phase of CSC transplantation may contribute to the early CSC-engraftment and late regeneration process of cardiovascular-lineage cells, we investigated the presence of *lacZ*$^+$ donor cells at day 7 and characterized their individual phenotypes 4 weeks after transplantation. As shown in Fig. 8A, the frequency of *lacZ*$^+$ cells observed 7 days post cell transfer was significantly lower in Sca-1 KD CSC grafts compared with NTG-CSC transplantation, resulting in substantially insufficient cardiovascular regeneration within the ischemic regions 4 weeks after CSC transplantation (Fig. 8B-D).

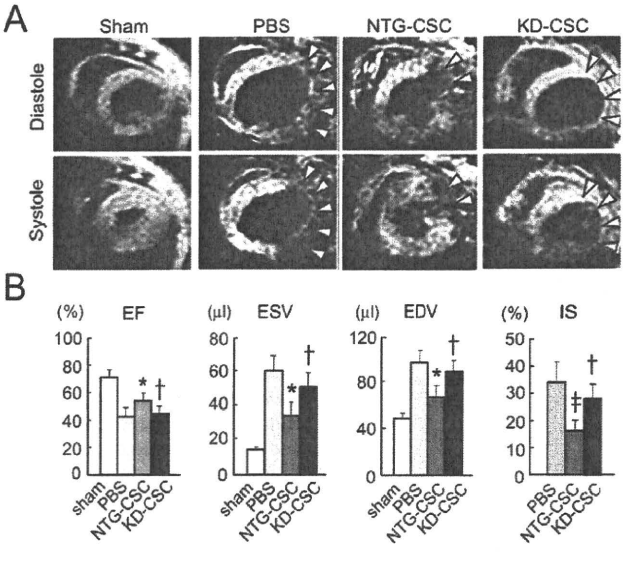

Fig. 6. Sca-1 KD CSC transplantation fails to prevent cardiac remodeling after myocardial infarction. (A,B) WT mice received transplantation of either NTG- or Sca-1 KD mice-derived CSCs 1 hour after infarction. Cardiac MRI was performed 4 weeks after CSC transplantation (n=8). Arrowheads indicate akinetic regions. White bars, sham-operated. Myocardial infarction with PBS injection (light gray bars), NTG-CSC (C6, dark gray bars) or Sca-1 KD-CSC (C1, black bars) transplantation are shown. *P<0.05 vs PBS; †P<0.05 versus NTG-CSC; ‡P<0.01 versus PBS injection. EF, ejection fraction; ESV, end-systolic volume; EDV, end-diastolic volume; IS, infarcted size.

Sca-1 KD CSC transplantation fails to prevent myocardial apoptosis and limits angiogenesis, partially due to the failure of paracrine effector secretion

Last, we assessed whether the loss of Sca-1 in transplanted

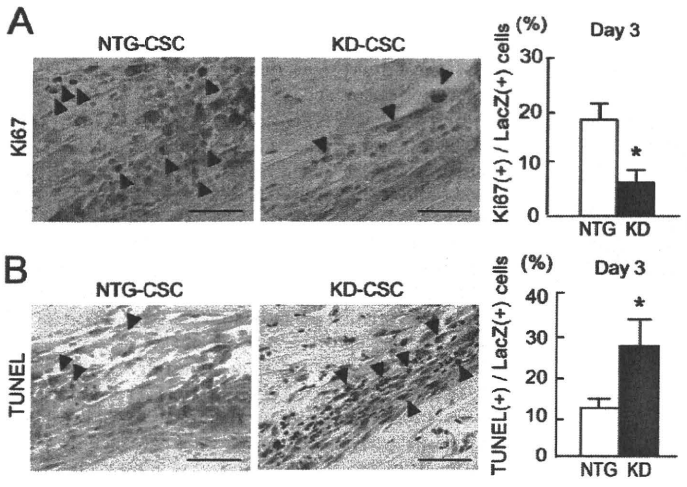

Fig. 7. Sca-1 transcripts are required for CSC proliferation and survival in vivo. (A) Immunohistochemistry of transplanted *lacZ*$^+$ cells 3 days after infarction. Transplanted *lacZ*$^+$ cells entering cell cycle were detected as Ki67-positive cells (arrowheads) (n=6). Myocardial infarction transplanted with NTG-CSCs (C6) and Sca-1 KD CSCs (C1) are shown. *P<0.01 versus NTG. (B) Apoptotic features (arrowheads, brown nuclei) of *lacZ*$^+$ engrafted cells are shown at day 3 after NTG- or Sca-1 KD-CSC transplantation. *P<0.01 versus NTG-CSC transplantation (n=6). Bars, 50 μm in A,B.

CSCs affects myocardial apoptosis and angiogenesis. At day 3, transplantation of Sca-1 KD CSCs resulted in a high level of myocardial apoptosis in the ungrafted area of the infarcted border zone, whereas fewer TUNEL-positive cells were observed in NTG-CSC-injected hearts (Fig. 9A). Furthermore, transplantation of Sca-1 KD CSCs failed to improve capillary density 2 weeks after infarction in the ischemic region as compared with NTG-CSC injection (Fig. 9B). To explore the molecular mechanisms of Sca-1-mediated myocardial apoptosis and neoangiogenesis, we then oxygen-starved CSCs for 8 hours and measured the levels of mRNA for secreted paracrine factors by RT-PCR. As shown in Fig. 9C, downregulation of hepatocyte growth factor (HGF) in Sca-1 KD CSCs was evident at baseline normoxia. After hypoxia, a greater increase in the expression of VEGF and HGF was observed in NTG-CSCs compared with that in Sca-1 KD CSCs. The expression pattern of insulin-like growth factor-1 (IGF1) under normoxic and hypoxic conditions was comparable in CSCs from NTG and Sca-1 KD hearts.

Discussion

Recent reports have shown that clonogenic CSCs reside in

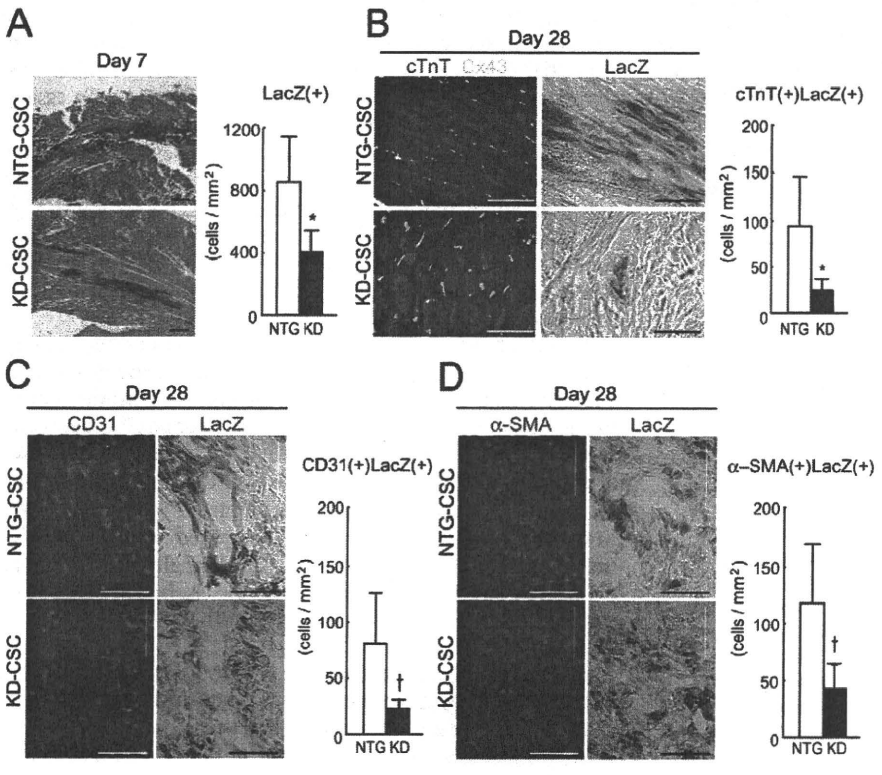

Fig. 8. Loss of Sca-1 transcripts in clonal CSC transplantation shows less donor-cell engraftment, resulting in the decrease in late cardiovascular regeneration. (A) Engrafted *lacZ*$^+$ cells in NTG (C6)- and Sca-1 KD-CSC (C1)-transplanted hearts at day 7 after infarction. Sections were counterstained using H&E. (B-D) The representative images and frequencies of cardiomyocytes (cardiac troponin-T, red), and endothelial (CD31) and smooth muscle cells (α-SMA) in *lacZ*$^+$ cells at day 28 are shown (n=6). Note that differentiated *lacZ*$^+$ cardiomyocytes co-express connexin-43 (yellow). Bars, 100 μm in A; 20 μm in B; 50 μm in C,D.

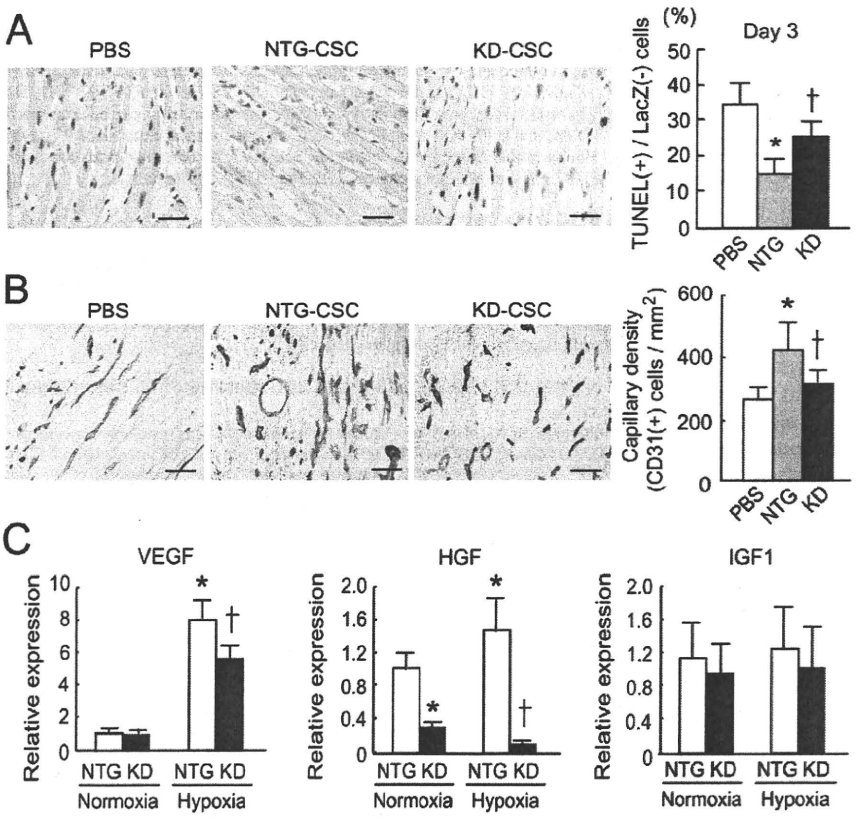

Fig. 9. Transplantation of Sca-1 KD CSCs fails to prevent myocardial apoptosis and limits neoangiogenesis after myocardial infarction partially due to the failure of paracrine effector secretion. (A) TUNEL staining revealed the apoptotic cardiomyocytes in the border zone of PBS-treated, NTG (C6)- and Sca-1 KD-CSC (C1)-transplanted hearts at day 3; (n=6). *P<0.01 vs PBS. †P<0.01 vs NTG. (B) Capillary density of infarcted border zone of transplanted hearts at day 14 after myocardial infarction. Capillary density was measured by staining of CD31 (brown) and corrected by the area analyzed. (n=8). *P<0.01 vs PBS-treated mice; †P<0.01 vs NTG-CSC-transplanted mice. Bars, 50 μm in A,B. (C) Relative mRNA expression levels of VEGF, HGF, and IGF1 normalized by 18S expression in NTG- and Sca-1 KD-CSCs under normoxic and hypoxic conditions (n=7). *P<0.01 vs NTG-CSCs under normoxia; †P<0.01 vs NTG-CSCs under hypoxia.

mammalian hearts, judging on the basis of specific cell-surface markers which are also expressed by hematopoietic and endothelial progenitor cells (Beltrami et al., 2003; Linke et al., 2005). Using an unbiased approach, our study has demonstrated that clonally proliferated CSCs express Sca-1 with ES cell-like and mesenchymal-cell-like characteristics, and are associated with TERT expression.

Our results, showing low expression of KIT in clonal *Kit*$^+$ CSCs, differ from the findings of some previous studies (Linke et al., 2005; Messina et al., 2004) but are consistent with those of recent reports about the adult heart (Fazel et al., 2006; Gude et al., 2006; Matsuura et al., 2004; Oh et al., 2003; Pfister et al., 2005; Tateishi et al., 2007). The reasons for this discrepancy are unclear. However, retrospective analysis data that directly sorted TERT-expressing cells from TERT-EGFP hearts (that were genetically isolated without the modification by cell culture) have shown that the majority of heart-resident TERT-positive cells could be identified via the expression of Sca-1. This implies that our findings were neither the result of intra-clonal variability nor due to contamination by cardiac fibroblasts during cell expansion. Recent report demonstrated that the expression levels of Sca-1 and KIT appear to be changed during myocardial maturation in ES cells (Wu et al., 2006).

Mesenchymal stem cells have been isolated from many tissues, including human heart (da Silva Meirelles et al., 2006; Tateishi et al., 2007). It is notable that CSCs expressed general characteristics of mesenchymal stem cells according to the analysis of cell-surface markers and partially showed the embryonic factors, as previously reported in clonal amniotic fluid-derived mesenchymal stem cells (Tsai et al., 2006). These observations indicated that the epithelial-mesenchymal transition (EMT) may occur in adult CSCs to produce proliferative precursors, which may undergo a reversible commitment into the directions of either mesenchymal or cardiac lineage, depending on the inductive conditions (Wessels and Perez-Pomares, 2004). Several reports suggest that the source of CSCs may include the neural crest (Tomita et al., 2005), primitive epicardial cells (Hay, 2005) or perivascular cells (da Silva Meirelles et al., 2006) through the EMT.

Regulating stem cell self-renewal is an essential feature of the niche where stem cells must be exposed to sufficient intrinsic-factors to maintain the proper stem cell number for the demands of tissue repair. We focused on Sca-1-mediated regulation in CSCs for the first time and found that normal Sca-1 function is associated with CSC proliferation and survival, contributing to early donor-cell engraftment and late cardiovascular differentiation, which is consistent with the prevailing view of the role of Sca-1 in the ability of hematopoietic stem cells and bone-marrow-derived mesenchymal stem cells to self-replicate (Bonyadi et al., 2003; Ito et al., 2003). Although the function of Sca-1 in skeletal muscle progenitors was not consistent with our observations in CSCs, the cell fate decision might be cell-type specific and/or age dependent (Mitchell et al., 2005). The mode of action of *Lin*$^-$*-Kit*$^+$ cells in the heart or bone marrow has been intensively investigated in gain- (Dawn et al., 2006; Urbanek et al., 2005a)

and loss-of-function experiments, and the function of these cells was validated by bone marrow reconstitution studies to completely rescue the defective cardiac repair in c-kit mutant mice after infarction (Ayach et al., 2006; Fazel et al., 2006), consistent with the lack of cardiac decompensation after pressure-overload in c-kit mutant mice (Hara et al., 2002) and our present observation indicating the rarity of c-kit$^+$ cells in TERT-expressing CSCs.

Sca-1 was originally identified as an antigen upregulated in activated lymphocytes, and was shown to be linked to the lipid bilayer as a glycosyl phosphatidylinositol (PtdIns)-anchored protein that activates cell signaling via mediators such as Akt (Reiser et al., 1986). The proliferation of CSCs appears to be dependent on the capacity of the cells to undergo cell cycle progression through the phosphorylation of Akt in response to EGF and bFGF stimulation, as observed in neural stem cells (Groszer et al., 2006). Our observations are supported by two independent gain-of-function studies demonstrating that the nuclear-targeting of Akt leads to the rapid expansion of comparatively rare *Kit*$^+$ CSCs in the postnatal heart (Gude et al., 2006), and ex-vivo transduction of Akt to bone marrow-derived MSCs can functionally repair the ischemic myocardium through the upregulation of secreted paracrine effectors (Gnecchi et al., 2006; Jiang et al., 2006). Consistent with these studies, our present study also demonstrated that the functional improvement of damaged myocardium after CSCs transplantation was attenuated by Sca-1 KD, in which new vessel formation and inhibition of myocardial apoptosis by release of angiogenic growth factors and myocyte regeneration by grafted CSCs were severely impaired.

Taken together, our results suggest that Sca-1 is expressed in the majority of intrinsic CSCs in the adult heart, which have characteristics of ES-like and mesenchymal-like cells, and implicate the role of Sca-1 in CSC maintenance and function. Sca-1-mediated signaling is important in CSC development in normal circumstances and its beneficial effect might be involved the responses to hypoxic and ischemic conditions. The cardioprotective effect of CSC transplantation that we have shown here indicates that Sca-1-mediated ligand responses may participate in the production of angiogenic and antiapoptotic paracrine effectors, consistent with recent observations demonstrating that induction of VEGF and HGF activates bone marrow-derived mesenchymal stem cells through PI 3-kinase–Akt pathway (Forte et al., 2006; Okuyama et al., 2006). It will be of interest to assess the gene expression profile in CSCs by targeting Sca-1 transcripts to identify the factors responsible for optimizing CSC therapy in heart failure.

Materials and Methods

Clonal isolation and culture of CSCs

Hearts from 6-week-old to-12-week-old GFP transgenic mice (provided by M. Okabe, Osaka University Medical School) (Okabe et al., 1997), Sca-1 KD mice or NTG mice were excised and were perfused with cold PBS to remove the blood cells. The tissues were washed twice, and aortic and pulmonary vessels were removed from the hearts. The dissected hearts were minced, and digested twice for 20 minutes at 37°C with 0.2% type II collagenase and 0.01% DNAse I (Worthington Biochemical Corp, NJ). The cells were passed through a 40-μm filter to remove the debris and were plated into 25-cm^2 dishes in DMEM (Invitrogen) for 30 minutes to allow fibroblasts to adhere. The non-adherent cells were collected and size-fractionated with a 30-70% Percoll gradient to obtain single-cell suspensions by removal of mature cardiomyocytes. For clonal analysis, the resulting cell suspensions were plated in 96-well plates at 1 cell per 100 μl by the limiting dilution technique (Yoon et al., 2005) with serum-free growth medium: DMEM/F12 containing B27 supplement, 20 ng/ml EGF (Sigma), and 40 ng/ml bFGF (Promega). Wells were visually inspected 24 hours after plating to exclude those containing more than one cell per well; then, clones derived from a single cell were further cultivated. On day 14, clonally expanded CSCs from single cells were cultured in low-serum medium consisting of growth medium supplemented with 1×B27 supplement, 2% FBS, and 10 ng/ml leukemia inhibitory factor (CHEMICON). At 60-70% confluence, cells from individual clones were serially reseeded in six-well plates, 25-cm^2, 75-cm^2 and 175-cm^2 flasks for further expansion. Hypoxic conditions were created by incubating cells at 37°C in a CO_2 multi-gas incubator (ASTEC) with an atmosphere of 5% CO_2 and 95% N_2 for 8 hours.

CSC differentiation

For cardiac differentiation analysis, single-cell-derived CSCs were cultured in differentiation medium containing 10% FBS, insulin-transferrin-selenium, and 10 nM dexamethasone (Sigma) for 14 days. Differentiation medium consisting of DMEM/F12 supplemented with 10 ng/ml VEGF or 50 ng/ml PDGF-BB (both from R&D Systems) and 10% FBS was used to induce endothelial and smooth muscle cell differentiation for 14 days, respectively.

Construction of targeting vector and generation of transgenic mice

Full-length Sca-1 cDNA was cloned using the following primers: forward: 5′-CTCTGAGGATGGACACTTCT-3′, reverse: 5′-GGTCTGCAGGAGGACTGA-GC-3′. The 404-bp ds-RNA fragment targeting the N-terminus of Sca-1 was selectively amplified and subcloned into the pDECAP vector (Shinagawa and Ishii, 2003). The plasmid encoding EGFP driven by the mouse *Tert* promoter was provided by N. Hole (University of Durham) (Armstrong et al., 2000) and subcloned into the human growth hormone polyadenylation sequence. Each expression cassette was released and microinjected into the pronuclei of fertilized C57BL/6 oocytes. PCR analysis of tail DNA was used to identify founder transgenic mice.

Retroviral transduction of CSCs

To track cells after injection into the infarcted myocardium, CSCs were engineered to express the bacterial *lacZ* reporter gene. This was done by retroviral infection with a vector (pMSCV-LacZ) encoding the *lacZ* gene and a puromycin resistance gene. After selection with puromycin, the transduction efficiency was evaluated by X-gal staining.

FACS analysis and cell sorting

Single-cell suspensions were stained with the following antibodies: phycoerythrin (PE)-conjugated antibodies against Sca-1, KIT, CD45, CD44, CD90, CD31, CD73, CD106, CD34, CD13, CD29, and isotype control IgG (all from BD Biosciences). Allophycocyanin (APC)-conjugated goat anti-rat IgG was used to detect rat anti-mouse CD105 (Southern Biotech). Dead cells were eliminated using propidium iodide (Sigma) and 10,000 to 50,000 events were collected per sample using a FACS Calibur flow cytometer (BD Biosciences). Bone marrow cells were flushed from the tibiae and femurs of 6-week-old to 12-week-old C57BL/6 mice and compared (with or without collagenase and filtration) (Oh et al., 2003). Single-cell suspensions were harvested from TERT-EGFP transgenic and NTG hearts as the method for CSC preparation, and the EGFP-positive cells were analyzed and sorted on BD FACSAria (Becton Dickinson).

RT-PCR and telomerase activity

Total RNA was prepared from cultured cells using TRIzol (Invitrogen) and cDNA was generated with the SuperScript III First-Strand Synthesis System (Invitrogen). PCR reactions were performed with gene-specific primers. Primer sequences are available on request. To evaluate VEGF, HGF, and IGF1 expression, cDNA was subjected to 40 rounds of amplification (ABI PRISM 7700, Applied Biosystems) with Assay-on-Demand™ primer-probes sets (Applied Biosystems). The mRNA levels were expressed relative to an endogenous control (18S RNA) and the fold-increase in the respective groups versus normoxia NTG-CSCs was calculated. Telomerase activity of single-cell-derived CSCs was measured using a TRAP assay kit, TRAPEZE (CHEMICON), as previously described (Oh et al., 2001).

Calcium transient

Cells were washed three times with 1 mM Ca^{2+} Tyrode's solution as previously described (Kaneko et al., 2000), additional 15 minutes incubation with 1 mM Ca^{2+} Tyrode's containing 1 mM probenecid at 37°C was performed to allow hydrolysis of acetoxymethyl esters within the cells. Fluorescence imaging was performed at 24°C using a fixed-stage microscope (BX50WI, Olympus, Japan) equipped with a multi-pinhole-type confocal scanning system (CSU-21, Yokogawa, Japan). Digitized fluorescence signals were analyzed with Image J software.

Western blotting

Whole protein lysates were extracted with lysis buffer: 50 mM Tris-HCl (pH 7.4), 150 mM NaCl, 0.25% sodium deoxycholate, 1 mM EDTA, 1% Nonidet P-40, 1 mM PMSF and protease inhibitor (PIERCE). For phosphorylation of Akt, ERK1/2, JNK1/2 and p38, 1 mM Na_3VO_4 and 1 mM NaF were added. Transferred